J Therm Anal Calorim (2017) 130:2145–2156
DOI 10.1007/s10973-017-6761-y

Dynamic DSC curing kinetics and thermogravimetric study of epoxy resin of 9,9′-bis(4-hydroxyphenyl)anthrone-10

Jabal D. Thanki[1,2] · **Parsotam H. Parsania**[1]

Received: 22 September 2016 / Accepted: 5 October 2017 / Published online: 20 October 2017

Abstract Dynamic DSC curing kinetics of epoxy resin of 9,9′-bis(4-hydroxyphenyl) anthrone-10 (EAN) was carried out at 5, 10, 15 and 20 °C min^{-1} heating rates in nitrogen atmosphere using 4,4′-diaminodiphenylsulfone (DDS), 4,4′-diaminodiphenylmethane (DDM) and tetrahydrophthalicanhydride (THPA) hardeners. Peak exotherms shifted toward higher temperature range with increasing heating rate. DSC data were analyzed by Ozawa, Kissinger and Flynn–Wall–Ozawa methods to derive activation energy (E_a) and frequency factor (A). Observed trend in E_a and A is EAN-DDS > EAN > EAN-THPA > EAN-DDM. For EAN-amine systems, both E_a and A decreased with increasing conversion and for EAN-THPA they increased up to 30% conversion and then decreased slowly with increasing conversion. Friedman plots showed autocatalytic nature of the EAN-hardener systems. Autocatalytic nature is due to dehydration of secondary alcohol groups with simultaneous formation of allylic double bonds. EAN-THPA showed 1.34 and 0.34, respectively, for n and m orders of kinetics. The validity of kinetic model was performed by simulation analysis using obtained kinetic constants for EAN-THPA. Experimental and calculated curves are in agreement between $\alpha = 0.2$–0.6. Thermogravimetric study at 10 °C min^{-1} heating rate in nitrogen atmosphere revealed that cured resins (310–337 °C) are more thermally stable than thermally cured EAN (279 °C) and followed either one- or two-step degradation kinetics.

✉ Parsotam H. Parsania
phparsania22@gmail.com

[1] Department of Chemistry, Polymer Chemistry Division, Saurashtra University, Rajkot 360005, India

[2] Department of Chemistry, Marwadi University, Rajkot 360003, India

Keywords Epoxy resin · Curing kinetics · Autocatalysis · Thermal stability · Kinetic parameters

Introduction

Industrially epoxy resins are very important thermoset materials [1] and find their usefulness in the field of coatings [2, 3], high-performance composites [4], insulating materials [5], microelectronics [6] and encapsulants [7]. For excellent engineering performance, materials must satisfy high-temperature performance [8], creep resistance [9], high stiffness [10], high electrical and mechanical properties [11]. Superior thermal, mechanical, electrical, chemical resistance, adhesive and low shrinkage properties of epoxy resins make them high-performance materials for various applications. For optimum process parameters and high production rate with satisfactory properties, precise understanding of curing process is essential [12]. Curing kinetics is useful for the comparison of curing behavior of different compositions of different matrices, catalysts, fillers, additives, etc. [13]. Both degree of cure and reaction rate strongly affect processing and physical properties of the cured epoxy resins [14].

Differential scanning calorimetry (DSC) is the most useful technique in understanding curing kinetics and key process parameters [15]. Recently, several investigators had used DSC technique to understand non-autocatalytic and autocatalytic curing of epoxy resins by different curing agents [12–27] and discussed autocatalysis mechanism. With the advancement of the technology, several researchers had attempted to enhance thermal stability of epoxy resins by introducing various aromatic ring structures such as biphenyl, naphthalene, fluorine, anthrone, heterocycles, etc., in the epoxy skeleton [28–30].

To the best of our knowledge, no work has been reported on dynamic DSC curing kinetics of epoxy resin of 9,9′-bis(4-hydroxyphenyl)anthrone-10 (Scheme-1). In this study, an attempt has been made to understand dynamic DSC curing kinetics of epoxy resin of 9,9′-bis(4-hydroxyphenyl)anthrone-10 at four different heating rates using three different curing agents such as 4,4′-diaminodiphenylsulphone (DDS), 4,4′-diaminodiphenylmethane (DDM) and tetrahydrophthalicanhydride (THPA). The derived results are discussed in light of the structure of curing agents on kinetic behavior.

Experimental

Materials

The materials used in this study were of laboratory grade and were purified prior to their use [31]. 4,4′-Diaminodiphenylmethane (DDM) (Spectrochem, Mumbai), 4,4′-diaminodiphenylsufone (DDS) (National Chemicals, Vadodara) and tetrahydrophthalicanhydride (THPA) (Merck, Germany) were used as received. Epoxy resin of 9,9′-bis(4-hydroxyphenyl)anthrone-10 (EAN) was synthesized and purified according to our recent publication [32]. Epoxy equivalent weight of the resin used in the present study was 940.

Measurements

Dynamic differential scanning calorimetric (DSC) curing study of EAN was studied on a Shimadzu DSC60 at four different heating rates: 5, 10, 15 and 20 °C min^{-1} in N_2 atmosphere (100 mL min^{-1}). DSC was calibrated by pure indium metal prior to the study of EAN. The samples were prepared thoroughly by grinding 20% of hardeners and EAN. Known mass of the samples was taken in aluminum pans covered by aluminum lids and sealed using a crimper. DSC curves were scanned over temperature range from room temperature to 400 °C. TG curves of cured and uncured samples were scanned on a Shimadzu DTG 60H at 10 °C min^{-1} heating rate in N_2 atmosphere.

Curing kinetics

Many kinetic models such as *n*th-order reaction, the autocatalytic reaction and the diffusion control models have been developed to investigate the curing kinetics of the epoxy resins [17–20]. All kinetic studies rely on the fundamental equation that governs the rate of conversion at constant temperature as a function of the concentration of the reactants [21]:

$$\frac{d\alpha}{dt} = \beta\frac{d\alpha}{dT} = kf(\alpha) \quad (1)$$

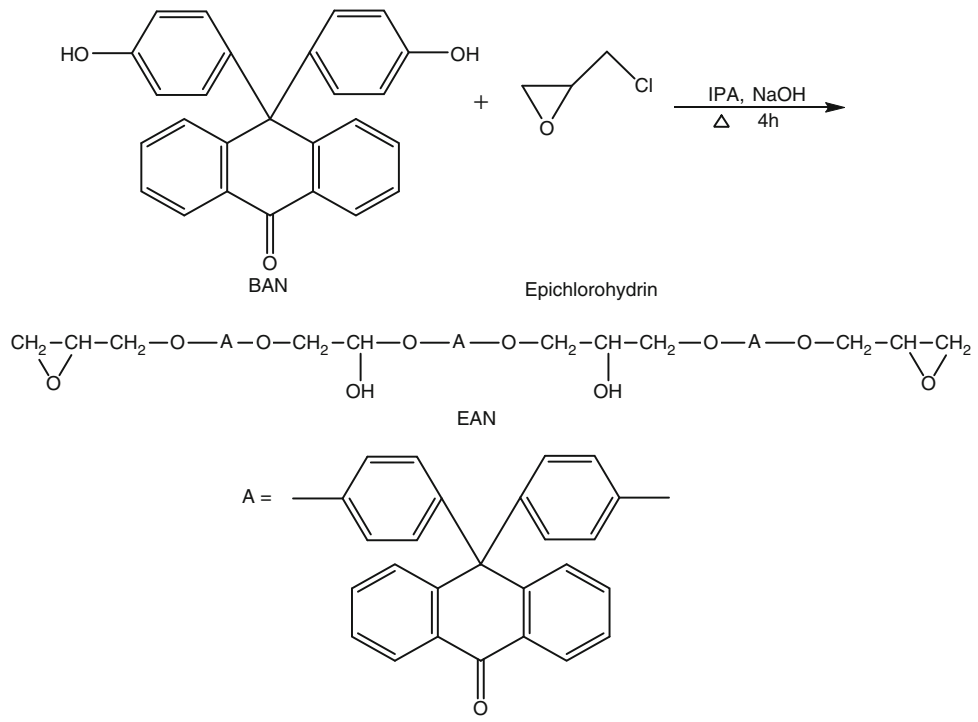

Scheme 1 Epoxy resin of 9,9′-bis(4-hydroxyphenyl) anthrone-10 (EAN)

where α is the degree of cure, $\beta = dT/dt$ is the heating rate, k is a temperature-dependent reaction rate constant, $f(\alpha)$ is the differential conversion function, and it depends on the reaction mechanism. Generally, k assumes to have the Arrhenius form:

$$k = Ae^{-E_a/RT} \quad (2)$$

$$f(\alpha) = (1-\alpha)^n \quad (3)$$

$$A = \frac{E_a \beta}{RT^2} e^{E_a/RT} \quad (4)$$

where A is the pre-exponential factor, E_a is the activation energy, R is the gas constant, T is the absolute temperature and n is the order of reaction.

Nonisothermal method is more precise method to evaluate the curing kinetic parameters. This method is very simple and rapid for the determination of kinetic parameters. The isothermal method renders the destabilization of the DSC heat flow at the beginning of the measurement, which leads to experimental errors. The two methods cover different temperature domains as discussed by Sbirrazzuoli et al. [22]. The shape of curing peak, the number of peaks and/or shoulders in the isothermal and nonisothermal DSC curves may be different. Although there is only a single peak in the isothermal DSC curve, a peak and a shoulder may appear in the nonisothermal DSC curve. Consequently, the kinetic parameters obtained from an isothermal cure study may not be good in predicting the nonisothermal curing behaviors [23]. Nonisothermal method involves either single or multiple dynamic temperatures scans in the study of the curing reactions of thermosets [24–26]. Kissinger, Ozawa, Friedman and Flynn–Wall–Ozawa methods are widely used to study dynamic kinetics of thermosetting polymers.

The Kissinger method

The Kissinger method is widely used for the estimation of the kinetic parameters such as E_a and A from dynamic DSC data. At the peak temperature, the rate of curing is maximum [33]. Using peak temperature data, activation energy can be determined according to Eq. 5:

$$\ln \frac{\beta}{T_p^2} = \ln \frac{Q_p AR}{E_a} - \frac{E_a}{RT} \quad (5)$$

where

$$Q_P = -\frac{df(\alpha)}{d\alpha} = \alpha_p \quad (6)$$

The plot of $\ln \beta/T_p^2$ against $1/T$ should be a straight line with slope equal to $-E_a/R$.

The Ozawa method

The Ozawa method [34] relates the logarithm of the heating rate and the inverse of the exothermic peak temperature.

$$\ln \beta = \ln\left(\frac{AE_a}{R}\right) - \ln f(\alpha) - 5.331 - 1.052\frac{E_a}{RT} \quad (7)$$

$$f(\alpha) = \int_0^{\alpha} \frac{d\alpha}{f(\alpha)} \quad (8)$$

where $f(\alpha)$ is a constant function. The plot of $\ln \beta$ against $1/T$ should be a straight line with slope equal to $-1.052\ E_a/R$.

Isoconversional method

The isoconversional method assumes that both of the activation energy (E_a) and pre-exponential factor (A) are the functions of the degree of curing (α). In addition, the isoconversional approach can be used to evaluate both simple and complex chemical reactions. The significance of this technique is that no kinetic rate expression is assumed for the data evaluation [34]. Two different isoconversional methods are as follows.

Friedman method

This method is one of the isoconversional methods based on the assumption that kinetic parameters E_a and A vary with extent of the reaction (α) [35]. The Friedman method for nth-order reaction is based on Eq. 9:

$$\ln \frac{d\alpha}{dt} = \ln \beta \frac{d\alpha}{dT} = \ln[Af(\alpha)] - \frac{E_a}{RT} \quad (9)$$

Upon substituting Eq. 4 in Eq. 9 gives Eq. 10:

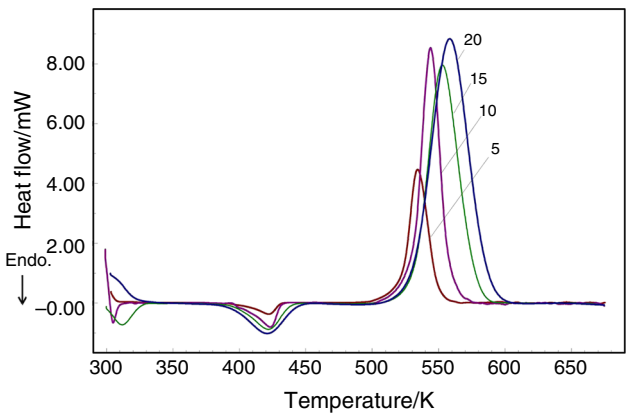

Fig. 1 DSC curves for EAN at 5, 10, 15 and 20 °C min^{-1} heating rates in nitrogen atmosphere

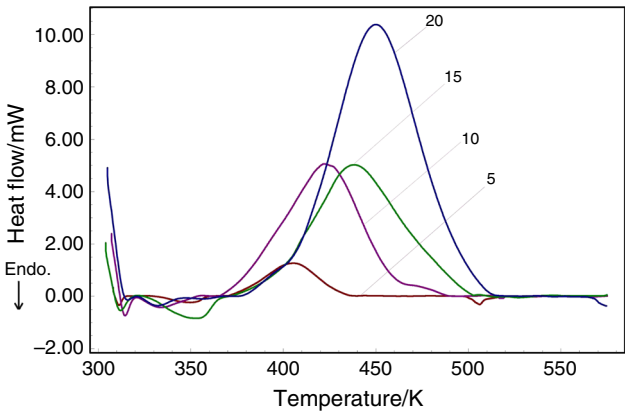

Fig. 2 DSC curves for EAN-DDM at 5, 10, 15 and 20 °C min^{-1} heating rates in nitrogen atmosphere

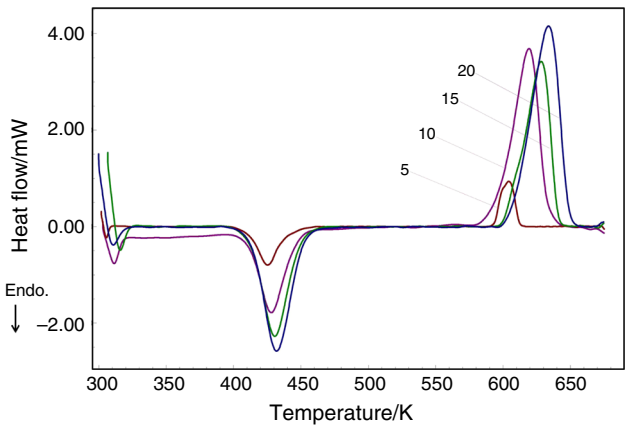

Fig. 3 DSC curves for EAN-DDS at 5, 10, 15 and 20 °C min^{-1} heating rates in nitrogen atmosphere

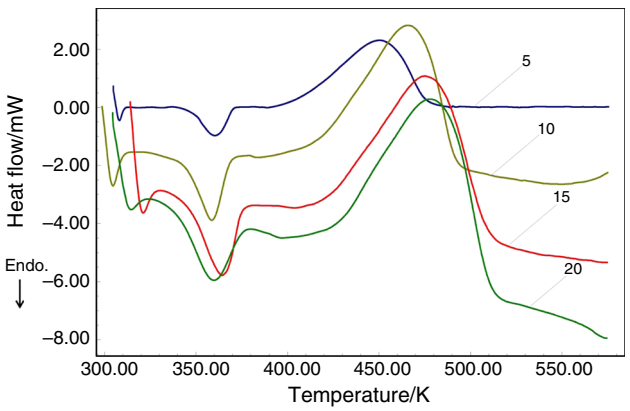

Fig. 4 DSC curves for EAN-THPA at 5, 10, 15 and 20 °C min^{-1} heating rates in nitrogen atmosphere

$$\ln[Af(\alpha)] = \ln\frac{d\alpha}{dt} + \frac{E_a}{RT} = \ln A + n\ln(1-\alpha) \quad (10)$$

The values of ln [Af (α)] can be obtained from the known values of ln [dα/dt] and E_a/RT. Therefore, the plot of ln [Af (α)] and ln(1 − α) yields a straight line with slope equal to n and the intercept equal to ln A.

The Flynn–Wall–Ozawa method

The isoconversional integral method was proposed independently by Flynn, Wall and Ozawa [36] using Doyle's approximation of the temperature integral.

$$\ln\beta = \ln\left(\frac{AE_a}{R}\right) - \ln g(\alpha) - 5.331 - 1.052\frac{E_a}{RT} \quad (11)$$

$$g(\alpha) = \int_0^{\alpha} \frac{d\alpha}{f(\alpha)} \quad (12)$$

where $g(\alpha)$ is the integral conversion function. The isoconversional method assumes that both of the activation energy and pre-exponential factors are the functions of the degree of curing. In addition, the isoconversional approach can be used to evaluate both simple and complex chemical reactions. The significance of this technique is that no kinetic rate expression is assumed for the data evaluation [37].

For a constant degree of conversion α, the plot of ln β versus $1/T$ should be a straight line with slope equal to − 1.052 E_a/R. The apparent activation energy derived from the Flynn–Wall–Ozawa method is more reliable than that of the Friedman method owing to its integrating character exhibiting less sensitivity to noise than the Friedman method. The later, however, provides a better visual separation of more reaction steps as well as information concerning the existence of an autocatalytically activated process [38]. The advantage of nonisothermal method is that they do not require prior knowledge of the reaction mechanism in order to quantify kinetic parameters [39]. Pre-exponential factor (A) can be determined according to Eq. 4.

Kinetic models

The mechanism of nonisothermal curing kinetics for epoxy resins is based on nth-order and autocatalytic models [40]. In case of nth-order model, conversion rate is proportional to concentration of unreacted material. The reaction rate is dependent only on the amount of unreacted material remaining, and the reaction products are not involved in the reaction. On the other hand, autocatalyzed model assumes that at least one of the reaction products is involved in propagating reaction and characterized by maximum degree of conversion between 20 and 60%. To predict the cure kinetics over the whole range of conversion, the Friedman isoconversional method can be employed for nonisothermal dynamic DSC data.

Table 1 Dynamic DSC curing data of EAN, EAN-DDM, EAN-DDS and EAN-THPA at multiple heating rates

System	Heating rate/ °C min^{-1}	T_i/ °C	T_p/ °C	T_f/ °C	dH/J g^{-1}
EAN	5	523.35	534.25	548.95	297.3
	10	531.05	543.85	556.95	275.0
	15	532.35	552.95	576.72	262.3
	20	531.45	558.35	585.95	290.4
EAN-DDM	5	376.55	405.55	431.05	119.6
	10	377.55	422.05	455.45	200.5
	15	397.75	438.35	489.85	183.2
	20	406.75	450.05	495.95	209.4
EAN-DDS	5	593.65	604.25	611.95	37.1
	10	596.15	619.25	632.35	115.2
	15	605.35	628.45	640.05	72.9
	20	606.85	633.65	648.15	93.0
EAN-THPA	5	406.25	450.45	474.05	170.3
	10	418.15	465.75	491.45	182.2
	15	423.95	475.05	508.75	176.7
	20	425.75	478.05	510.45	149.0

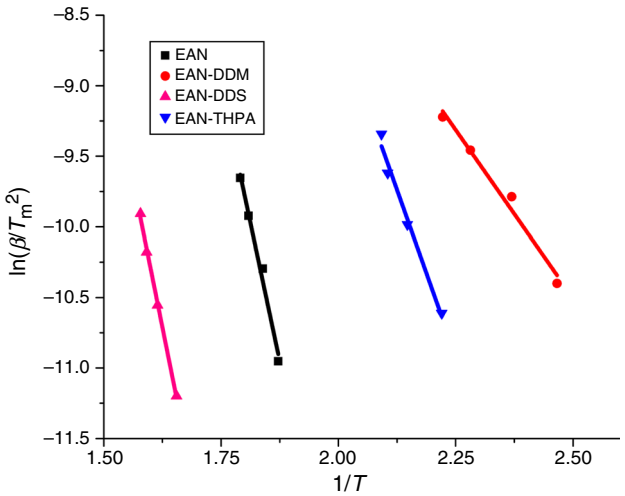

Fig. 5 Kissinger plots for EAN, EAN-DDM, EAN-DDS and EAN-THPA

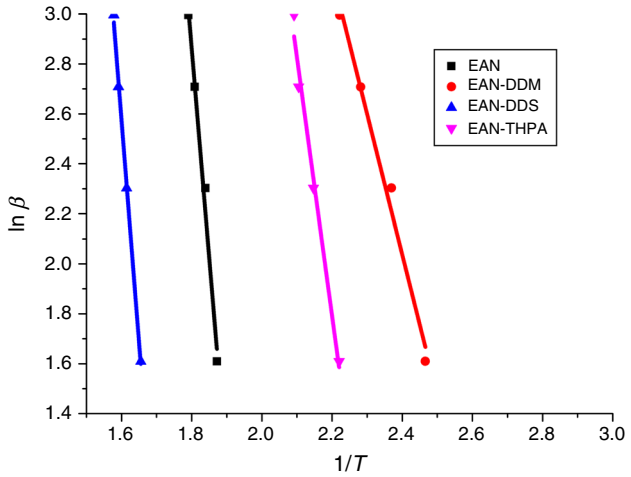

Fig. 6 Ozawa plots for EAN, EAN-DDM, EAN-DDS and EAN-THPA

For nth-order kinetics, the rate of the reaction can be expressed as:

$$\frac{d\alpha}{dt} = A(1-\alpha)^{n} e^{-E_a/RT} \quad (13)$$

For autocatalyzed reaction, the rate of reaction can be expressed as

$$\frac{d\alpha}{dt} = A\alpha^{m}(1-\alpha)^{n} e^{-E_a/RT} \quad (14)$$

where n and m are the orders of the two independent reactions. According to nth-order kinetic model, the maximum reaction rate will be observed at $t = 0$ and for autocatalytic model, the reaction rate is zero initially and attains the maximum value at some intermediate conversion.

Logarithmic forms of Eqs. 13 and 14 can be expressed as

Table 2 Activation energies of EAN, EAN-DDM, EAN-DDS and EAN-THPA derived according to Kissinger and Ozawa methods

Method	E_a/kJ mol^{-1}			
	EAN	EAN-DDM	EAN-DDS	EAN-THPA
Kissinger	130.43	39.61	137.82	78.24
Ozawa	132.61	44.41	140.77	81.7

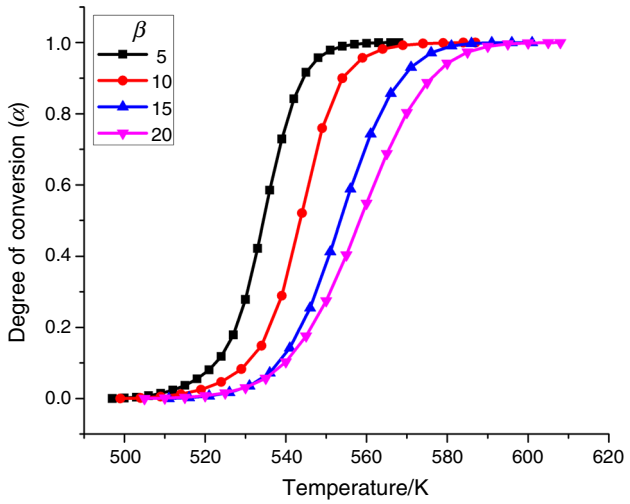

Fig. 7 Plots of degree of conversion against temperature at 5, 10, 15 and 20 °C min^{-1} for EAN

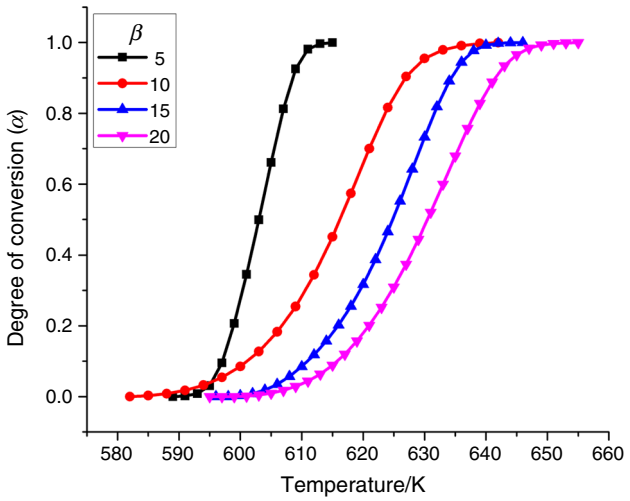

Fig. 9 Plots of degree of conversion against temperature at 5, 10, 15 and 20 °C min^{-1} for EAN-DDS

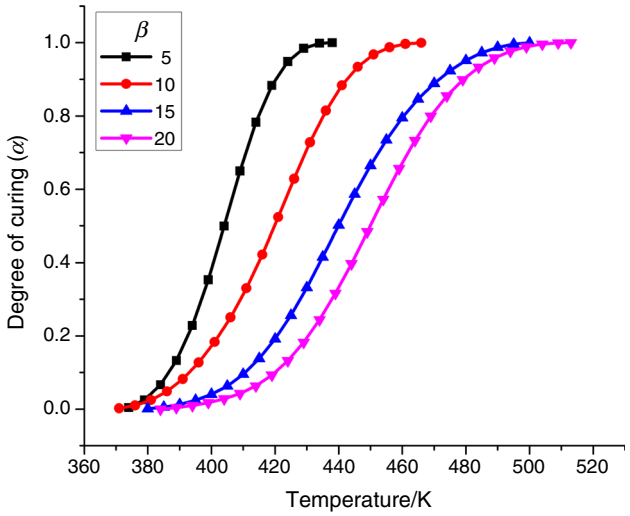

Fig. 8 Plots of degree of conversion against temperature at 5, 10, 15 and 20 °C min^{-1} for EAN-DDM

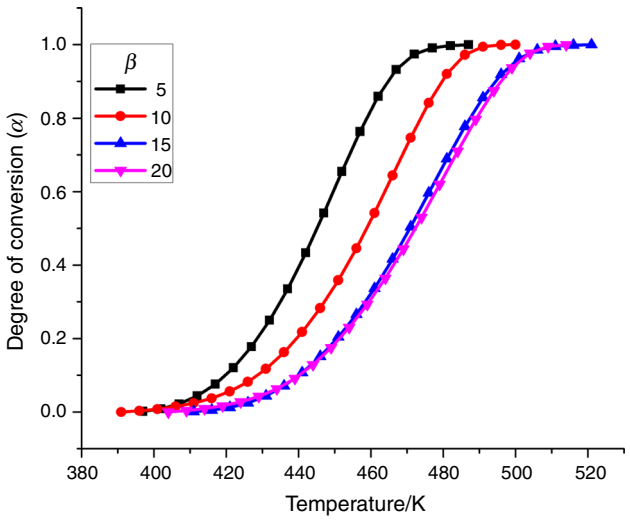

Fig. 10 Plots of degree of conversion against temperature at 5, 10, 15 and 20 °C min^{-1} for EAN-THPA

$$\ln\frac{d\alpha}{dt} = \ln A - \frac{E_a}{RT} + n\ln(1-\alpha) \quad (15)$$

$$\ln\frac{d\alpha}{dt} = \ln A - \frac{E_a}{RT} + n\ln(1-\alpha) + m\ln\alpha \quad (16)$$

Equations 15 and 16 can be solved by multiple linear regression method. The dependent variable is ln dα/dt, and the independent variables are ln α, ln $(1-\alpha)$ and $1/T$. The values of A, m and n can be obtained using the average activation energy from Flynn–Wall–Ozawa method. The degree of curing is chosen between the beginning of the reaction and the maximum peak of degree of curing ($\alpha = 0.2$–0.6).

Results and discussion

DSC curves of EAN, EAN-DDM, EAN-DDS and EAN-THPA at four different heating rates: 5, 10, 15 and 20 °C min^{-1} in nitrogen atmosphere are presented in Figs. 1–4, respectively. From Figs. 1–4, it is observed that melting and peak exotherms are shifted toward higher-temperature range with increasing heating rate. The onset of curing temperature (T_o), peak maximum temperature (T_p) and curing range is reported in Table 1. Heat of curing at each heating rate for each sample was determined by the measurement of area under exothermic peak (dH_T) and is also reported in Table 1. From Table 1, it is observed that no systematic trend was observed for dH with increasing β.

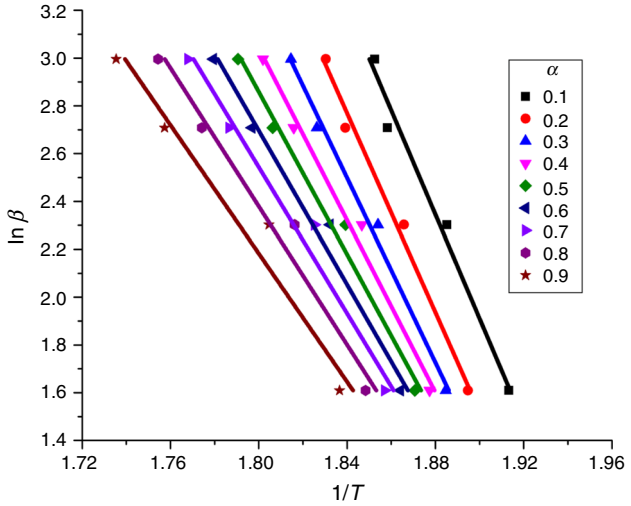

Fig. 11 Flynn–Wall–Ozawa plots for EAN at various degrees of curing

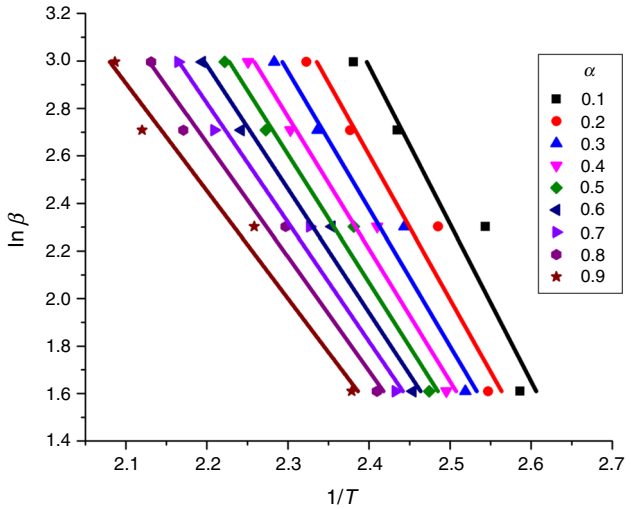

Fig. 12 Flynn–Wall–Ozawa plots for EAN-DDM at various degrees of curing

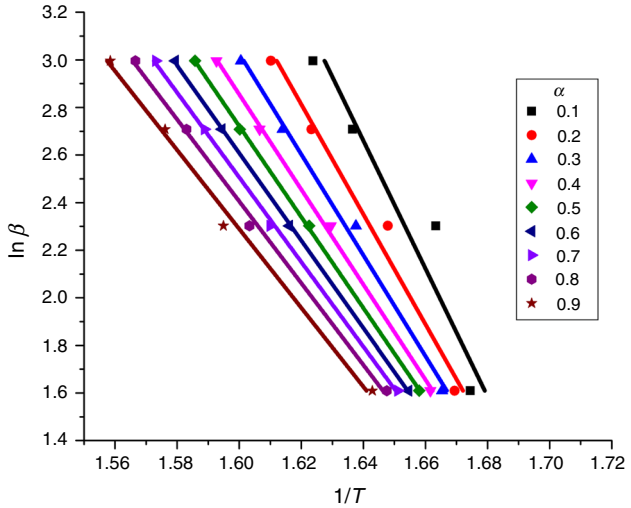

Fig. 13 Flynn–Wall–Ozawa plots for EAN-DDS at various degrees of curing

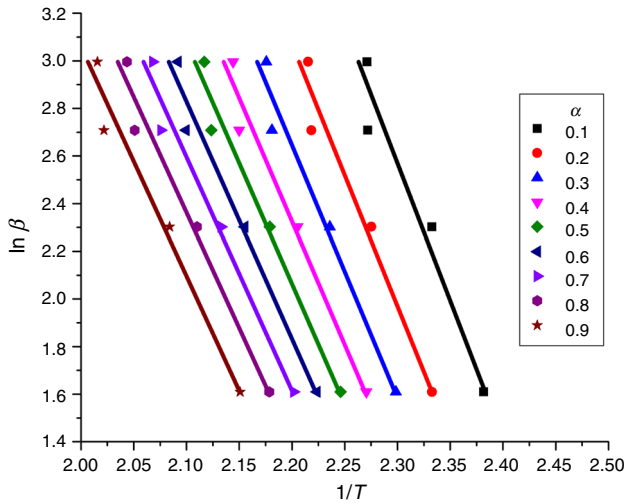

Fig. 14 Flynn–Wall–Ozawa plots for EAN-THPA at various degrees of curing

In order to evaluate E_a, DSC data were analyzed according to Kissinger (Eq. 5) and Ozawa (Eq. 7) methods from which it is observed that E_a values derived according to Ozawa method are somewhat higher than that of the Kissinger method due to approximation made in Ozawa method. Kissinger and Ozawa plots of all the four samples are shown in Figs. 5 and 6, respectively. The values of E_a were derived from the slopes and are shown in Table 2. Observed trend of E_a is EAN-DDS > EAN > EAN-THPA > EAN-DDM due to different nature of matrix and hardeners. The low values of E_a for EAN-DDM and EAN-THPA indicated flexible nature of cured resin, while high values of E_a for EAN and EAN-DDS suggested rigid nature of the cured resin.

In order to evaluate E_a and A, DSC data were analyzed according to Flynn–Wall–Ozawa (Eq. 11) isoconversional method. For that various degrees of curing (α) for a given sample and for a given heating rate were evaluated by measuring total area (dH_T) under the DSC curve and partial area (dH) at definite temperature. The degree of curing (α) is the ratio of dH to dH_T. Degree of conversion against temperature plots for these samples at multiple heating rates are shown in Figs. 7–10 from which it is observed that in the beginning and toward the end of the curing reaction $\alpha-T$ correlation is nonlinear in accordance with epoxies studied by several investigators [12–27]. Flynn–Wall–Ozawa isoconversional curves for EAN, EAN-DDM,

EAN-DDS and EAN-THPA are shown in Figs. 11–14, respectively. Derived values of E_a and A are presented in Tables 3–6 from which it is observed that both E_a and A are decreased considerably with increasing degree of curing for EAN, EAN-DDM and EAN-DDS, while they increased slowly up to $\alpha = 0.3$ and then decreased with increasing α values for EAN-THPA system. Observed trend in E_a and A is EAN-DDS > EAN > EAN-THPA > EAN-DDM. For epoxy-amine systems, decrease in E_a and A with increasing α is due to intermolecular cross-linking breaking resulting in increasing chain flexibility. Such behavior is also observed in epoxy-amine systems [22, 27, 41, 42].

Table 3 Activation energies and pre-exponential factors derived for EAN according to Flynn–Wall–Ozawa method

Degree of curing	E_a/kJ mol^{-1}	A/s^{-1}			
		5	10	15	20
0.1	168.90	4.7×10^{14}	5.2×10^{14}	4.4×10^{14}	5.1×10^{14}
0.2	162.80	7.6×10^{13}	8.4×10^{13}	7.2×10^{13}	8.0×10^{13}
0.3	151.27	4.2×10^{12}	4.7×10^{12}	4.1×10^{12}	4.3×10^{12}
0.4	140.38	2.9×10^{11}	3.3×10^{11}	2.9×10^{11}	3.0×10^{11}
0.5	132.26	3.9×10^{10}	4.6×10^{10}	3.9×10^{10}	4.0×10^{10}
0.6	124.80	6.2×1^{09}	7.4×10^{09}	6.3×10^{09}	6.3×10^{09}
0.7	117.83	1.1×1^{09}	1.3×10^{09}	1.1×10^{09}	1.1×10^{09}
0.8	110.90	1.9×1^{08}	2.4×10^{08}	2.0×10^{08}	2.0×10^{08}
0.9	101.87	2.0×1^{07}	2.7×10^{07}	2.1×10^{07}	2.1×10^{07}

Table 4 Activation energies and pre-exponential factors derived for EAN-DDM according to Flynn–Wall–Ozawa method

Degree of curing	E_a/kJ mol^{-1}	A/s^{-1}			
		5	10	15	20
0.1	47.66	8.8×10^{03}	1.3×10^{04}	9.8×10^{03}	9.2×10^{03}
0.2	45.37	3.2×10^{03}	4.4×10^{03}	3.3×10^{03}	3.1×10^{03}
0.3	43.96	1.7×10^{03}	2.2×10^{03}	1.7×10^{03}	1.6×10^{03}
0.4	42.81	1.0×10^{03}	1.2×10^{03}	9.6×10^{02}	9.4×10^{02}
0.5	41.67	6.2×10^{02}	7.2×10^{02}	5.7×10^{02}	5.7×10^{02}
0.6	40.37	3.6×10^{02}	4.1×10^{02}	3.3×10^{02}	3.3×10^{02}
0.7	38.91	2.0×10^{02}	2.3×10^{02}	1.8×10^{02}	1.8×10^{02}
0.8	37.15	1.0×10^{02}	1.1×10^{02}	8.6×10^{01}	9.2×10^{01}
0.9	34.95	4.4×10^{01}	4.7×10^{01}	3.5×10^{01}	3.9×10^{01}

Table 5 Activation energies and pre-exponential factors derived for EAN-DDS according to Flynn–Wall–Ozawa method

Degree of curing	E_a/kJ mol^{-1}	A/s^{-1}			
		5	10	15	20
0.1	194.35	5.4×10^{14}	8.3×10^{14}	6.4×10^{14}	6.3×10^{14}
0.2	178.62	1.9×10^{13}	2.3×10^{13}	2.0×10^{13}	2.0×10^{13}
0.3	166.45	1.4×10^{12}	1.5×10^{12}	1.4×10^{12}	1.4×10^{12}
0.4	157.67	2.1×10^{11}	2.2×10^{11}	2.1×10^{11}	2.1×10^{11}
0.5	151.07	5.0×10^{10}	5.1×10^{10}	4.9×10^{10}	5.0×10^{10}
0.6	145.42	1.5×10^{10}	1.4×10^{10}	1.4×10^{10}	1.4×10^{10}
0.7	140.51	5.0×1^{09}	4.8×10^{09}	4.9×10^{09}	4.9×10^{09}
0.8	135.54	1.7×1^{09}	1.6×10^{09}	1.6×10^{09}	1.6×10^{09}
0.9	130.23	5.3×1^{08}	4.7×10^{08}	5.1×10^{08}	5.1×10^{08}

Table 6 Activation energies and pre-exponential factors derived for EAN-THPA according to Flynn–Wall–Ozawa method

Degree of curing	E_a/kJ mol^{-1}	A/s^{-1}			
		5	10	15	20
0.1	71.82	3.5×10^{06}	4.4×10^{06}	3.7×10^{06}	4.9×10^{06}
0.2	74.71	5.2×10^{06}	5.9×10^{06}	5.0×10^{06}	6.5×10^{06}
0.3	75.16	4.2×10^{06}	4.5×10^{06}	3.9×10^{06}	5.0×10^{06}
0.4	75.07	3.1×10^{06}	3.2×10^{06}	2.8×10^{06}	3.5×10^{06}
0.5	74.80	2.3×10^{06}	2.3×10^{06}	2.0×10^{06}	2.5×10^{06}
0.6	74.46	1.6×10^{06}	1.7×10^{06}	1.4×10^{06}	1.8×10^{06}
0.7	74.00	1.2×10^{06}	1.2×10^{06}	1.0×10^{06}	1.2×10^{06}
0.8	73.60	8.3×10^{05}	8.5×10^{05}	7.1×10^{06}	8.9×10^{05}
0.9	73.41	6.0×10^{05}	6.3×10^{05}	5.1×10^{06}	6.4×10^{05}

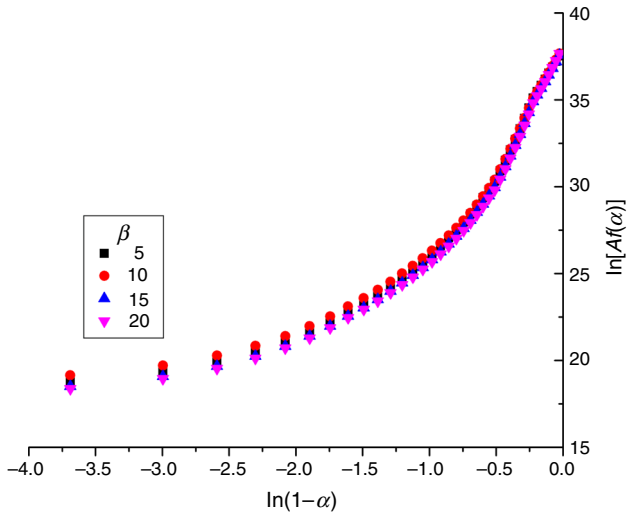

Fig. 15 Plots of ln [$Af(\alpha)$] against ln(1 − α) for EAN at 5, 10, 15 and 20 °C min^{-1} heating rates

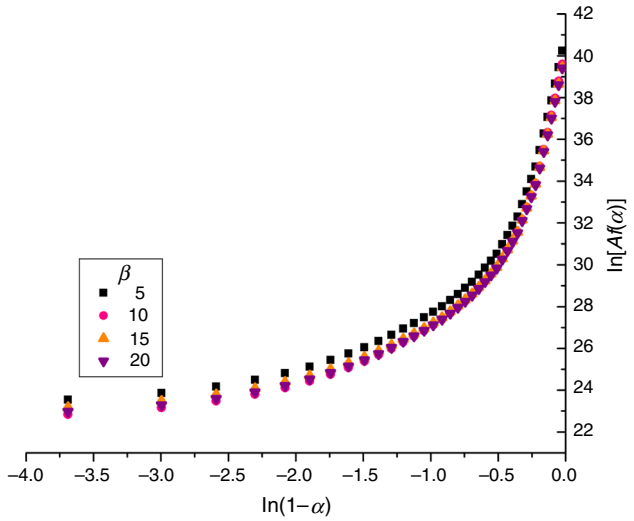

Fig. 17 Plots of ln [$Af(\alpha)$] against ln(1 − α) for EAN-DDS at 5, 10, 15 and 20 °C min^{-1} heating rates

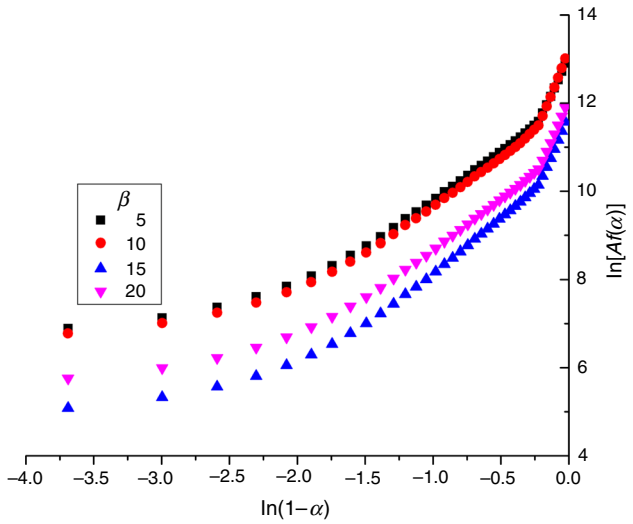

Fig. 16 Plots of ln [$Af(\alpha)$] against ln(1 − α) for EAN-DDM at 5, 10, 15 and 20 °C min^{-1} heating rates

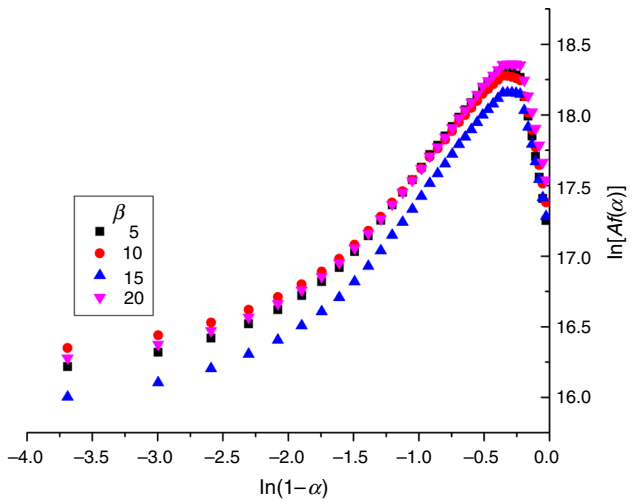

Fig. 18 Plots of ln [$Af(\alpha)$] against ln(1 − α) for EAN-THPA at 5, 10, 15 and 20 °C min^{-1} heating rates

Table 7 Order of the reactions derived according to Friedman's method for EAN-THPA

Reaction order	Heating rate/ °C min^{-1}				Mean value
	5	10	15	20	
n	1.19	1.15	1.46	1.38	1.3
m	0.32	0.26	0.42	0.35	0.34

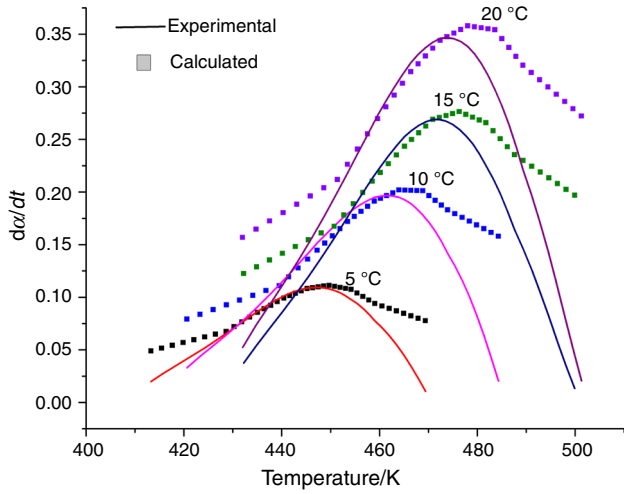

Fig. 19 Simulated conversion and experimental curves for EAN-THPA at 5, 10, 15 and 20 °C min^{-1} heating rates

Increasing values for E_a and A for EAN-THPA systems ($\alpha < 0.4$) indicated further cross-linking reaction of double bonds in THPA ring or thermal polymerization of allylic double bonds formed as a result of dehydration of secondary alcoholic groups. Thus, for epoxy-amine systems dependency of E_a with α is observed, which suggested that curing mechanism is kinetically complex.

Friedman method is an important tool in understanding autocatalytic mechanism. DSC data for all the systems were analyzed by Friedman method (Eq. 16). The Friedman plots for EAN, EAN-DDM, EAN-DDS and EAN-THPA are shown in Figs. 15–18 from which it is observed that nonlinear increase in ln [A dα/dt] with ln ($1 - \alpha$) for epoxy-amine systems and a maximum ($\alpha = 0.3$) for EAN-THPA systems implied autocatalytic nature of the reaction kinetics. The values of n and m for EAN-THPA system are reported in Table 7 from which it is observed that nth and mth reaction orders are 1.34 and 0.34, respectively, i.e., they followed fractional-order curing kinetics.

In order to confirm the validity of the kinetic model used, simulated conversion curves at multiple heating rates were constructed using obtained kinetic constants for EAN-THPA. Simulated conversion curves along with experimental curves at multiple heating rates are presented in

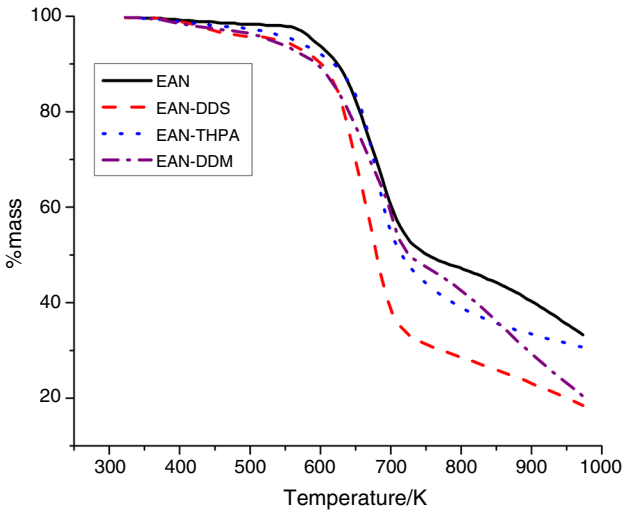

Fig. 20 Plots of % mass against temperature for EAN, EAN-DDM, EAN-DDS and EAN-THPA at 10 °C min^{-1} heating rate under N_2 atmosphere

Fig. 19 from which it is observed that the calculated and experimental curves are in good agreement between $\alpha = 0.2$ and 0.6. At higher degree of conversion, i.e., after onset of vitrification, the observed deviation is probably due to change in curing mechanism (diffusion controlled) [43]. At lower degree of conversion, the observed deviation is due to slow rate of curing and then after catalytic effect led to agreement between calculated and experimental results. In case of EAN-DDM and EAN-DDS, peak maxima were not observed in ln [$Af(\alpha)$] against ln ($1 - \alpha$) curves, and therefore, simulation analysis was not performed.

TGA curves of EAN, EAN-DDM, EAN-DDS and EAN-THPA at the heating rate 10 °C min^{-1} in nitrogen atmosphere are presented in Fig. 20 from which it is observed that EAN-DDM and EAN-DDS followed apparently single-step degradation, while EAN and EAN-THPA followed two-step degradation kinetics. Initial decomposition temperature T_o, decomposition range, the % mass loss involved and the % residue remained at 700 °C are reported in Table 8. Observed thermal stability order of cured resin is EAN-DDS > EAN-DDM > EAN-THPA > EAN. A considerable amount of residue left at 700 °C (14.6–33.5%) confirmed the formation of highly cross-linked products. Degradation process of a polymer is a complex process and involves a variety of reactions, namely cross-linking, branching, rearrangement, etc. Ether, hydroxyl, ester/amide linkages are weak linkages in the cured resin, which degrade selectively to form new products which further degrade at elevated temperatures. Considerably higher residue at 700 °C confirmed the formation of highly cross-linked materials.

Table 8 TG data of EAN, EAN-DDS, EAN-DDM and EAN-THPA cured resins

Parameter	EAN	EAN-DDM	EAN-DDS	EAN-THPA	
T_o/K	552.4	595.2	609.7	583.1	
Decomposition range/K	552–775	595–730	609–736	583–748	763–933
% Mass loss	49.3	57.5	46.3	17.6	38.5
% Residue at 973 K	33.5	18.6	30.8	14.6	

Conclusions

Dynamic DSC curing study was carried out to understand autocatalytic behavior of epoxy-amines and epoxy-anhydride systems. Flynn–Wall–Ozawa method showed E_a and A order as EAN-DDS > EAN > EAN-THPA > EAN-DDM. Both E_a and A decreased with increasing conversion in case of epoxy-amine systems. Friedman's autocatalytic model showed autocatalytic behavior of resin-hardener systems. Simulated conversion and experimental curves are found in good agreement between $\alpha = 0.2$–0.6 for EAN-THPA. Cured and uncured resins showed good thermal stability. Observed thermal stability order is EAN-DDS > EAN-DDM > EAN-THPA > EAN.

Acknowledgements The authors are thankful to FIST-DST and SAP-UGC for their instrumental support and University Grants Commission—New Delhi, for Major Research Project grants (Sanction No. 42-246/2013).

References

1. Hu F, La Scala JJ, Sadler JM, Palmese GR. Synthesis and characterization of thermosetting furan-based epoxy systems. Macromolecules. 2014;47(10):3332–42.
2. Nie L, Burgess A, Ryan A. Moisture permeation in liquid crystalline epoxy thermosets. Macromol Chem Phys. 2013;214(2):225–35.
3. Qureshi SS, Zheng Z, Sarwar MI, Félix O, Decher G. Nanoprotective layer-by-layer coatings with epoxy components for enhancing abrasion resistance: toward robust multimaterial nanoscale films. ACS Nano. 2013;7(10):9336–44.
4. Wajid AS, Ahmed H, Das S, Irin F, Jankowski AF, Green MJ. High-performance pristine graphene/epoxy composites with enhanced mechanical and electrical properties. Macromol Mater Eng. 2013;298(3):339–47.
5. Hsiao M-C, Ma C-CM, Chiang J-C, Ho K-K, Chou T-Y, Xie X, Tsai C-H, Chang L-H, Hsieh C-K. Thermally conductive and electrically insulating epoxy nanocomposites with thermally reduced graphene oxide–silica hybrid nanosheets. Nanoscale. 2013;5(13):5863–71.
6. Liu Y-L, Chuo T-W. Self-healing polymers based on thermally reversible Diels-Alder chemistry. Polym Chem. 2013;4(7):2194–205.
7. Elkington D, Cooling N, Zhou X, Belcher W, Dastoor P. Single-step annealing and encapsulation for organic photovoltaics using an exothermically-setting encapsulant material. Sol Energy Mat Sol Cells. 2014;124:75–8.
8. Ma S, Liu X, Jiang Y, Tang Z, Zhang C, Zhu J. Bio-based epoxy resin from itaconic acid and its thermosets cured with anhydride and comonomers. Green Chem. 2013;15(1):245–54.
9. Li Y, Kessler MR. Creep-resistant behavior of self-reinforcing liquid crystalline epoxy resins. Polymer. 2014;55(8):2021–7.
10. Jin H, Mangun CL, Griffin AS, Moore JS, Sottos NR, White SR. Thermally stable autonomic healing in epoxy using a dual-microcapsule system. Adv Mater. 2014;26(2):282–7.
11. Li T, Zhang J, Wang H, Hu Z, Yu Y. High-performance light-emitting diodes encapsulated with silica-filled epoxy materials. ACS Appl Mater Interfaces. 2013;5(18):8968–81.
12. Alonso M, Oliet M, Garcia J, Rodriguez F, Echeverría J. Gelation and isoconversional kinetic analysis of lignin–phenol–formaldehyde resol resins cure. Chem Eng J. 2006;122(3):159–66.
13. Boey F, Qiang W. Experimental modeling of the cure kinetics of an epoxy-hexaanhydro-4-methylphthalicanhydride (MHHPA) system. Polymer. 2000;41(6):2081–94.
14. Francucci G, Cardona F, Manthey NW. Cure kinetics of an acrylated epoxidized hemp oil-based bioresin system. J Appl Polym Sci. 2013;128(3):2030–7.
15. Sbirrazzuoli N, Vyazovkin S, Mititelu A, Sladic C, Vincent L. A study of epoxy-amine cure kinetics by combining isoconversional analysis with temperature modulated DSC and dynamic rheometry. Macromol Chem Phys. 2003;204(15):1815–21.
16. Hu J, Shan J, Wen D, Liu X, Zhao J, Tong Z. Flame retardant, mechanical properties and curing kinetics of DOPO-based epoxy resins. Polym Degrad Stab. 2014;109:218–25.
17. Wan J, Gan B, Li C, Molina-Aldareguia J, Kalali EN, Wang X, Wang D-Y. A sustainable, eugenol-derived epoxy resin with high biobased content, modulus, hardness and low flammability: synthesis, curing kinetics and structure–property relationship. Chem Eng J. 2016;284:1080–93.
18. Lu MG, Shim MJ, Kim SW. Effect of cure behavior of an epoxy system: cure modeling. Polym Eng Sci. 1999;39:274–85.
19. Wan J, Li C, Bu Z-Y, Xu C-J, Li B-G, Fan H. A comparative study of epoxy resin cured with a linear diamine and a branched polyamine. Chem Eng J. 2012;188:160–72.
20. Yang T, Zhang C, Zhang J, Cheng J. The influence of tertiary amine accelerators on the curing behaviors of epoxy/anhydride systems. Thermochim Acta. 2014;577:11–6.
21. Wan J, Li C, Bu Z-Y, Fan H, Li B-G. Evaluating a four-directional benzene-centered aliphatic polyamine curing agent for epoxy resins. J Therm Anal Calorim. 2013;114(1):365–75.
22. Patel A, Maiorana A, Yue L, Gross RA, Manas-Zloczower I. Curing kinetics of biobased epoxies for tailored applications. Macromolecules. 2016;49(15):5315–24.
23. Hu J, Shan J, Zhao J, Tong Z. Isothermal curing kinetics of a flame retardant epoxy resin containing DOPO investigated by DSC and rheology. Thermochim Acta. 2016;632:56–63.
24. Li C, Fan H, Hu J, Li B. Novel silicone aliphatic amine curing agent for epoxy resin: 1, 3-bis (2-aminoethylaminomethyl) tetramethyldisiloxane. 2. Isothermal cure, and dynamic mechanical property. Thermochim Acta. 2012;549:132–9.

25. Yagneswaran S, Tomar N, Smith DW Jr. Non-isothermal curing kinetics of epoxy/mechanochemical devulcanized ground rubber tire (GRT) composites. Polym Bull. 2013;70(4):1337–51.
26. Abenojar J, Martínez M, Pantoja M, Velasco F, Del Real J. Epoxy composite reinforced with nano and micro SiC particles: curing kinetics and mechanical properties. J Adhes. 2012;88(4–6):418–34.
27. Ghumara RY, Adroja PP, Parsania PH. Synthesis, characterization, and dynamic DSC curing kinetics of novel epoxy resin of 2, 4, 6-tris (4-hydroxyphenyl)-1-3-5-triazine. J Therm Anal Calorim. 2013;114(2):873–81.
28. Xin J, Zhang P, Huang K, Zhang J. Study of green epoxy resins derived from renewable cinnamic acid and dipentene: synthesis, curing and properties. RSC Adv. 2014;4(17):8525–32.
29. Yu M, Zhou Z, Lu H, Li A, Bai R, Sun J, Ren M, Hu H. Curing kinetics and thermal properties of aromatic multifunctional epoxy resins. Polym Polym Compos. 2014;22(1):1–11.
30. Luda M, Balabanovich A, Zanetti M, Guaratto D. Thermal decomposition of fire retardant brominated epoxy resins cured with different nitrogen containing hardeners. Polym Degrad Stab. 2007;92(6):1088–100.
31. Vogel AI, Tatchell AR, Furnis BS, Hannaford AJ, Smith PWG. Vogel's textbook of practical organic chemistry. 5th ed. Boston: Addison Wesley Longman Ltd; 1998. p. 395.
32. Bhuva BD, Parsania PH. Studies on jute/glass/hybrid composites of polyurethane based on epoxy resin of 9, 9′-bis (4-hydroxy phenyl) anthrone-10 (EBAN) and PEG-200. J Appl Polym Sci. 2010;118(3):1469–75.
33. Yang G, Yuan Z, Yang Z, Zhang M. Nonisothermal curing kinetics of a novel polymer containing phenylsilylene and propargyl–hexafluorobisphenol a units. J Appl Polym Sci. 2013;127(4):3178–85.
34. Ozawa T. Kinetic analysis of derivative curves in thermal analysis. J Therm Anal Calorim. 1970;2(3):301–24.
35. Jubsilp C, Punson K, Takeichi T, Rimdusit S. Curing kinetics of benzoxazine–epoxy copolymer investigated by non-isothermal differential scanning calorimetry. Polym Degrad Stab. 2010;95(6):918–24.
36. Sbirrazzuoli N, Girault Y, Elégant L. Simulations for evaluation of kinetic methods in differential scanning calorimetry. Part 3: peak maximum evaluation methods and isoconversional methods. Thermochim Acta. 1997;293(1):25–37.
37. Kessler MR, White SR. Cure kinetics of the ring-opening metathesis polymerization of dicyclopentadiene. J Polym Sci Part A Polym Chem. 2002;40(14):2373–83.
38. Opfermann J, Kaisersberger E. An advantageous variant of the Ozawa–Flynn–Wall analysis. Thermochim Acta. 1992;203:167–75.
39. He Y. DSC and DEA studies of underfill curing kinetics. Thermochim Acta. 2001;367:101–6.
40. Huang X, Patham B. Experimental characterization of a curing thermoset epoxy-anhydride system-Isothermal and nonisothermal cure kinetics. J Appl Polym Sci. 2013;127(3):1959–66.
41. Lakho DA, Yao D, Cho K, Ishaq M, Wang Y. Study of the curing kinetics towards development of fast curing epoxy resins. Polym Plast Tech Eng. 2016;. doi:10.1080/03602559.2016.1185623.
42. Wang H, Liu B, Liu X, Zhang J, Xian M. Synthesis of biobased epoxy and curing agents using rosin and the study of cure reactions. Green Chem. 2008;10(11):1190–6.
43. Prime Bruce R. Chapter 5-Thermosets. In: Turi EA editor. Thermal characterization of polymeric materials. London: Academic Press; 1981. p. 435–569.